WALAILAK JOURNAL
http://wjst.wu.ac.th Engineering and Physical Sciences

Normal Mode Analysis of the Nonlinear Acoustic Wave Equation

Mohamed Ibrahim Ahmed OTHMAN[1], Mohamed Galal Sayed ALI[2,*] and Roushdi Mohamed FAROUK[1]

[1]*Department of Mathematics, Faculty of Science, Zagazig University, Zagazig, Egypt*
[2]*Department of Physics, Faculty of Science, Minia University, Egypt*

([*]Corresponding author's e-mail: m_i_othman@yahoo.com, mgalal09@yahoo.com)

Abstract

Second-harmonic generation in non-linear media is investigated. A normal mode analysis is proposed based on the Westervelt equation under the second-order approximation in nonlinear acoustics. This model takes into consideration attenuation, diffraction and nonlinear effects, together with dispersion. The fundamental and second harmonic is examined. The derived method is evaluated by 2-D analytical formulas which apply to tissue medium.

Keywords: Second harmonic, normal mode, tissue, nonlinear, acoustic

Introduction

The mechanism of nonlinear generation has been widely investigated and numerous model equations have been proposed under different conditions [1-4]. When ultrasound propagates in fluid medium due to nonlinearity in the equations of motion and state, the waveform distorts progressively and new frequency components are generated. Kopfner and Lemons [5] were the first to demonstrate second harmonic imaging in water using a specially tuned microscope at a fundamental frequency of 400 MHz. They noted improvements in both the resolution and the contrast of the second harmonic image compared to the fundamental. Rugar [6] found the spatial frequency response of images formed at nonlinear drive levels to be a factor of 1.4 better than those formed during conventional linear imaging. Also, the second-harmonic generation of the *n*th-order Bessel beam in the nonlinear medium has been investigated by [7]. The numerical model for calculating the acoustic field was based on KZK (Khokhlov-Zablotskaya-Kuznetsov) [8] equations, which is a parabolic approximation to the nonlinear wave equation for the system, and it provides both amplitude and phase information along the acoustic axis of the transducer. At long propagation distances, KZK solutions based on finite difference [9] or finite element method [10] distort signals unacceptably, as they use lower order space and time derivative approximations. Nonlinear wave equations in an attenuating tissue medium have been solved by pseudo-spectral methods [11].

In this paper, the wave equation can be written as a superposition of a homogeneous Helmholtz equation [12] according to fundamental components and an inhomogeneous Helmholtz equation according to the second harmonic. These 2 equations can be solved separately by using normal mode analysis. The normal mode method [13] provides high spatial accuracy, as it solves the nonlinear wave equation at every point in the 2-D spatial domain. Normal mode analysis can be employed to solve nonlinear acoustic wave equations analytically. The technique focuses on the description of a nonlinear model and discusses the conditions used under this technique. A simulation method for the forward propagation of an acoustic pressure wave in a medium with two-dimensional spatially-variable acoustic properties is presented.

The nonlinear propagation of ultrasound waves in an absorbing medium can be described by the following equation [3];

$$\nabla^2 p - \frac{1}{c_0^2}\frac{\partial^2 p}{\partial t^2} + \frac{\delta}{c_0^4}\frac{\partial^3 p}{\partial t^3} = -\frac{\beta}{\rho_0 c_0^4}\frac{\partial^2 p^2}{\partial t^2}. \tag{1}$$

where p, $\rho_0, c_0, \delta, \beta$ represent acoustic diffusivity medium density, sound speed, sound diffusivity, and coefficient of nonlinearity, respectively. The right hand side of Eq. (1) accounts for the harmonic generation and is considered to be a small correction to the linear wave equation. Assuming that $p = p_1 + p_2$, p_1 is the sound pressure at the fundamental frequency f and p_2 is the pressure for the second harmonic at frequency $2f$. The higher harmonics are neglected due to their much smaller amplitudes and higher attenuations. The pressure p_1 and p_2 can be described by Helmholtz equations as follows.

$$\nabla^2 p_1 + k_1^2 p_1 = 0, \tag{2}$$

$$\nabla^2 p_2 + k_2^2 p_2 = -\frac{2i\beta k^2}{\rho_0 c_0^2} p_1^2, \tag{3}$$

where

$$k_1^2 = k^2 - i\,\frac{\delta k^3}{c_0}, \tag{4}$$

$$k_2^2 = 4k^2 - i\,\frac{8\delta k^3}{c_0}, \tag{5}$$

and k = ω / c . Eqs. (2) and (3) are solved by the normal mode method.

Normal mode analysis

The solution of the considered physical variables can be decomposed in terms of normal modes as the following form;

$$[p_1, p_2](x, y, t) = [p_1^*, p_2^*](x)\exp(\omega t + iby), \tag{6}$$

where the angular frequency is ω, $i = \sqrt{-1}$, b is the wave number in the y - direction. Eq. (2) becomes;

$$\left(D^2 - b^2\right) p_1^*(x) + k_1^2 p_1^*(x) = 0 \tag{7}$$

where $D = \frac{d}{dx}$

$$\left(D^2 - m^2\right) p_1^* = 0, \tag{8}$$

where $m^2 = -b^2 + k_1^2$

The solution of Eq. (8) has the form;

$$p_1^*(x) = \sum_i^2 p_{1i}^*, \tag{9}$$

where $p_{1i}^*(x) = c_1 e^{r_i x}$,

r_i are the roots of the characteristic equation;

$$r_i^2 - m^2 = 0, \tag{10}$$

From Eqs. (6) and (8);

$$p_1(x, y, t) = c_1 e^{-mx} e^{(\omega t + jby)} \tag{11}$$

is obtained. The solution of the non-homogeneous Eq. (3) using the normal mode analysis can be described as;

$$\mathrm{p_2(x,y,t) = \{c_2 e^{-m_1 x} - \frac{2i\beta k^2 c_1^2}{\rho_0 c_0^2 \left[4m^2 - m_1^2\right]} e^{(-2mx + wt + iby)}\} e^{(\omega t + iby)}}, \tag{12}$$

The total pressure for the fundamental and first harmonic can be written as;

$$p(x, y, t) = p_1(x, y, t) + p_2(x, y, t). \tag{13}$$

The solution of $P_1(x, y, t)$ and $P_2(x, y, t)$ must be bounded as $x \to \infty$.

Boundary condition

$$\begin{aligned} &y = 0\,,\ \ x = 0\ \ ,\ p = p_0 \\ &y = 0\,,\ \ x = L\,,\ t = t_L\ \ ,\ p^* = p_L^*(\omega, b), \end{aligned} \tag{14}$$

$$c_1 = \frac{p_L^* - p_0^* e^{-m_1 L}}{\left\{(1 + He^{(-2mL + \omega t_L}) - (1 + H)e^{-m_1 L}\right\}}, \tag{15}$$

$$c_2 = p_0^* - \frac{(1 + H) p_L^* - p_0^* e^{-m_1 L}}{\left\{(1 + He^{(-2mL + \omega t_L}) - (1 + H)e^{-m_1 L}\right\}}, \tag{16}$$

where $H = -\frac{2i\beta k^2}{\rho_0 c_o^2 \left[4m^2 - m_1^2\right]}$

Computational results

To study the second harmonic phenomenon in the test medium, the theoretical acoustics wave Eqs. (11) and (12) can be applied. Using tissue as the medium, the parameters are given as follows,

$\rho = 1000\ Kg/m^3$, $c = 1500$ m/s, $f = 1$ MHz, $\beta = 4.4$ and the diffusivity (δ) can be expressed as a function of the absorption coefficient $\alpha\alpha$ with the equation $\delta = 2\alpha c^3/\omega^2$ (where w is the angular frequency)[14]. Let the wave peak amplitude be $p_0^* = 1$ KPa at the source (x = 0); the wave peak amplitude, in Eqs. (11) and (12), is simulated, versus the distance from the source. The result is shown in **Figure 1**. It is clear from this figure that the wave peak amplitude becomes smaller as it moves further from the source. It can also be noticed that in the pressure for the second harmonic, more attenuation can be observed at any given location. The results obtained by the proposed method are in good agreement with previously published data [14-16]. The total pressure for the fundamental and second harmonic is shown in **Figure 2**. A 2-D simulation can be considered in which the pressure varies in the x and y directions. **Figures 3** and **4** show the 2-D pressure computational for the second harmonic and fundamental respectively as a function in the x-y plane. **Figure 5** shows the 2-D total pressure on the x-y plane. From these figures, it can be seen that the pressure amplitude becomes smaller when moving in the x-y plane further from the source. Results show that difference in values obtained by linear and nonlinear propagation model grows with applied input acoustic pressure amplitude. After the initial increase of distortion, a stronger decrease of the higher frequencies occurs with the distance from the source, giving a more and more sinusoidal signal. The dominance of the non-linear attenuation becomes clear.

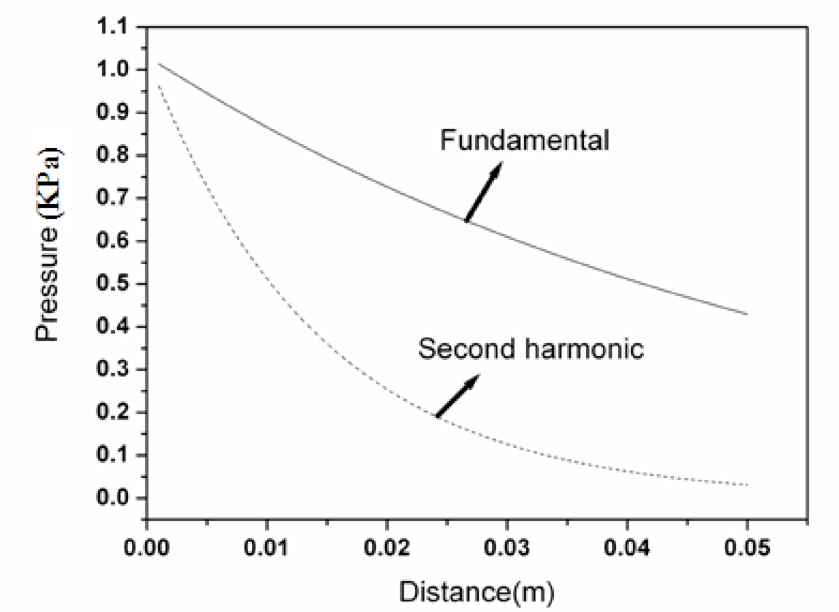

Figure 1 Pressure amplitude of fundamental and second harmonic as function of the distance from the origin.

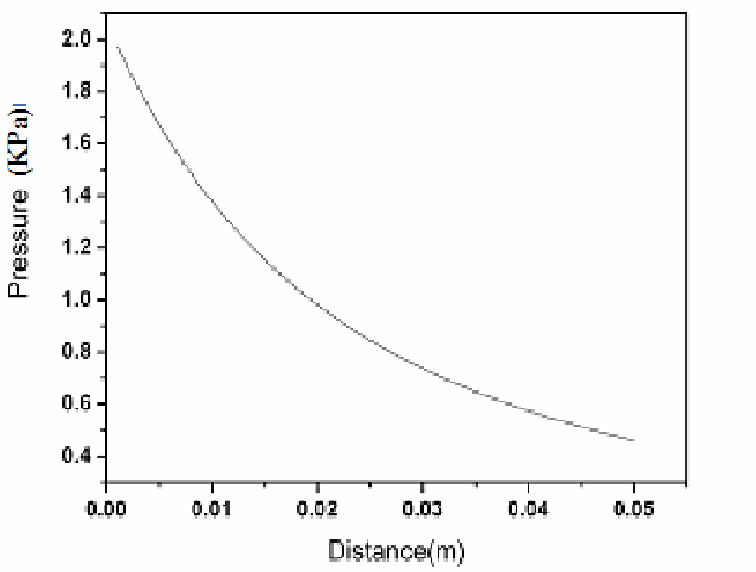

Figure 2 Total pressure amplitude as function of the distance from the origin.

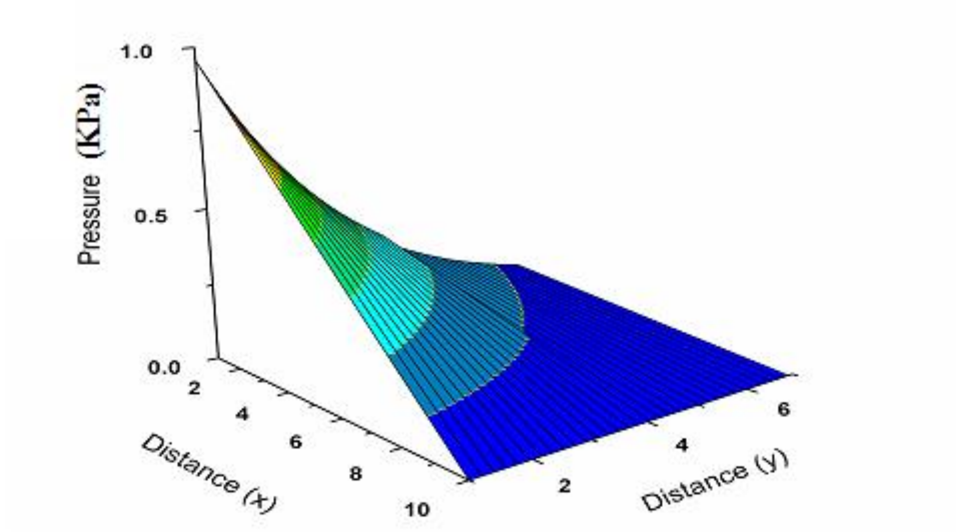

Figure 3 Pressure amplitude of second harmonic as function of plane x-y direction.

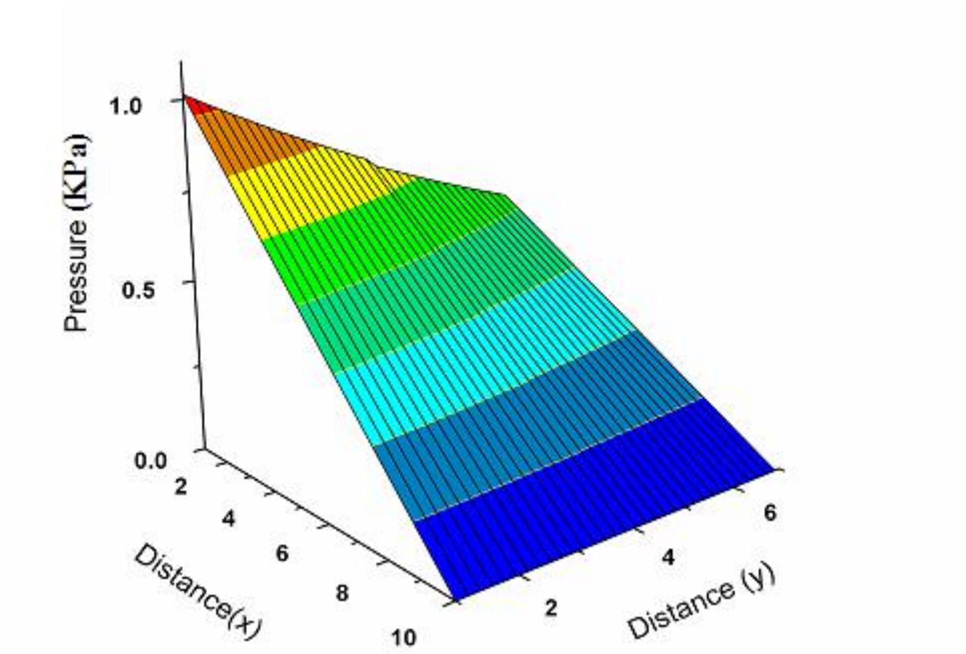

Figure 4 Pressure amplitude of fundamental as function of plane x-y direction.

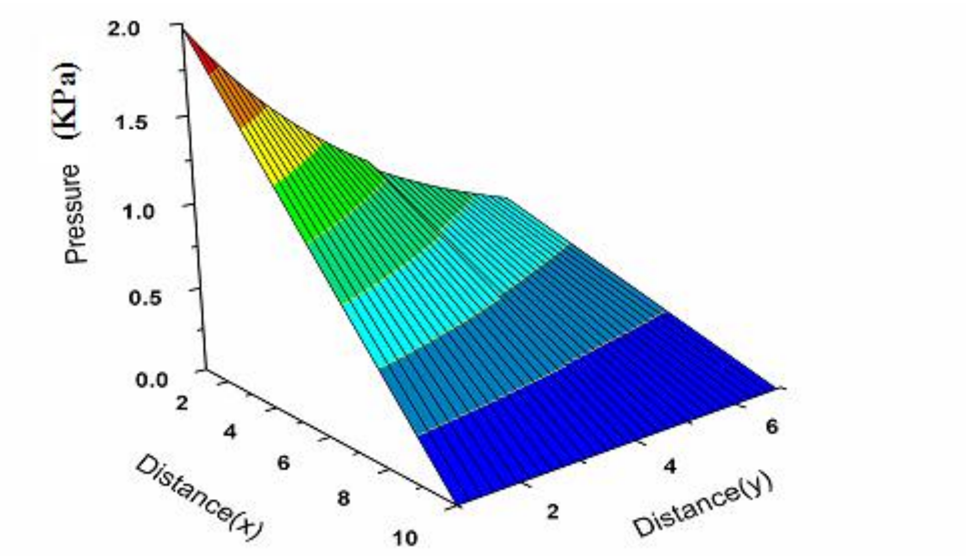

Figure 5 Total pressure amplitude as function of plane x-y direction.

Conclusions

In this paper the second harmonic generation arising from the nonlinear propagation of an ultrasonic wave in tissue medium was investigated. The analysis was based on a normal mode analysis which solved the nonlinear wave equation. The homogeneous and inhomogeneous Helmholtz equations were solved separately by using a normal mode analysis in the x-y plane. Loss effects were taken into account without approximations about the attenuation parameter value. The algorithm optimized the computing costs, and large propagation distances were considered. The second harmonic generation in inhomogeneity medium was analyzed. This technique has a number of attractive features, foremost of which is the speed and simplicity with which it can be designed and implemented.

References

[1] AD Mansfel'd, DA Mansfel'd and AM Reiman. Abilities of nonlinear acoustic methods in locating gas bubbles in biological tissues. *Acoust. Phys*. 2005; **51**, 209-17.

[2] CC Shen, CK Yeh, WS Chen and HW Wang. The effect of third harmonic transmit phasing on contrast agent responses for CTR improvement. *Phys. Med. Biol*. 2008; **53**, 6179-94.

[3] FA Duck. Nonlinear acoustics in diagnostic ultrasound. *Ultrasound Med. Biol.* 2002; **28**, 1-18.

[4] ND Londhe and RS Anand. Second harmonic field generation from a phased array transducer and its beam optimization. *Int. J. Recent Trends Eng.* 2009; **2**, 101-5.

[5] R Kompfner and RA Lemons. Nonlinear acoustic microscopy. *Appl. Phys. Lett.* 1976; **28**, 295-7.

[6] D Rugar. Resolution beyond the diffraction limit in the acoustic microscope: a nonlinear effect. *J. Acoust. Soc. Am*. 1984; **56**, 1338-46.

[7] D Ding and JY Lu. Second-harmonic generation of the *n*th-order Bessel beam. *Phys. Rev. E* 2000; **61**, 2038-41.

[8] YS Lee and MF Hamilton. Time-domain modeling of pulsed finite-amplitude sound beams. *J. Acoust. Soc. Am.* 1995; **97**, 906-17.

[9] X Yang and RO Cleveland. Time domain simulation of nonlinear acoustic beams generated by rectangular pistons with application to harmonic imaging. *J. Acoust. Soc. Am.* 2005; **117**, 113-23.

[10] MK Araz, CH Lee and A Lal. Finite Element modeling of ultrasonic separation at the microscale. *IEEE Trans. Ultrason. Ferroelectrics Freq. Contr*. 2004; **1**, 153-6.

[11] G Wojcik, B Fornberg, R Waag, L Carcione, J Mould, L Nikodym and T Driscoll. Pseudospectral methods for large-scale bioacoustic models. *IEEE Trans. Ultrason. Ferroelectrics Freq. Contr*. 1997; **2**, 1501-6.

[12] G Bao, GW Wei and S Zhao. Numerical solution of the Helmholtz equation with high wave numbers. *Int. J. Numer. Meth. Eng*. 2004; **59**, 389-408.

[13] MIA Othman, KH Lotfy and RM Farouk. Generalized thermo-micro-stretch elastic medium with temperature dependent properties for different theories. *Eng. Anal. Bound. Elem.* 2010; **34**, 229-37.

[14] L Demi and KWA Dongen. A contrast source method for nonlinear acoustic wave fields in media with spatially inhomogeneous attenuation. *J. Acoust. Soc. Am*. 2011, **129**, 1221-30.

[15] C Vanhille and C Campos-Pozuelo. Nonlinear ultrasonic resonators: A numerical analysis in the time domain. *Ultrasonics* 2006; **44**, 777-81.

[16] PT Christophera and KJ Parker. New approaches to nonlinear diffractive field Propagation. *J. Acoust. Soc. Am*. 1991; **90**, 499-88.